Electronic Supplementary Information

for

Highly-Efficient and Durable Carbon Nanotube-based Anode Electrocatalyst for Water Electrolyzer

Tsuyohiko Fujigaya, Yilei Shi, Jun Yang, Hua Li, Kohei Ito, Naotoshi Nakashima**

Table S1. Valence ratios of Ir determined from the XPS for MWNT/PBI/Ir, CB/PBI/Ir and CB/Ir and MWNT/PBI/IrO_x.

	Ir(0)	Ir(IV)
MWNT/PBI/Ir	86.4%	13.6%
CB/PBI/Ir	81.4 %	18.6%
CB/Ir	88.4%	11.6%
MWNT/PBI/IrOx	65.5%	34.5%

Table S2. Comparison of half-cell performance of OER between the present- and reported catalysts.

Sample	Ir-based mass activity (A g^{-1})		q^* (mC mg^{-1})	Durability† (hour)	Ref.
	@1.48 V vs. RHE	@1.51 V vs. RHE			
MWNT/PBI/IrOx	75	213	187	27	this work
CB/PBI/IrOx	89	235	209	6	
CB/IrOx	53	150	104	4	
ATO-supported $IrNiO_x$	—	92	—	20	S1
Ir nanodendrite supported on ATO	—	68	108	15	S2
Ir black	—	31	64	6	
Rutile IrO_2 nanoparticle	3	—	—	—	S3
Ir-Ni bimetallic nanoparticles	—	490	—	12	S4

†The durability of all the catalysts were evaluated by chronopotentiometry measurements at 1.0 mA cm^{-2}.

Table S3. Comparison of single-cell performance of PEMWEs between the present- and previously reported cells.

Cathode	Pt loading in cathode (mg cm^{-2})	Anode	Ir loading in anode (mg cm^{-2})	Electrolyte	Cell voltage @1 A cm^{-2} (V)	Ir-based mass activity @1.6 V (A g^{-1})	Ref.
Pt/CB	0.5	MWNT/PBI/Ir	0.5	Nafion117	1.647	1533	this work
Pt/CB	0.5	CB/PBI/Ir	0.5	Nafion117	1.779	992	
Pt/CB	0.4	ATO-supported Ir nanodentrite	1.0	Nafion212	1.653	690	S2
Pt/CB	0.5	IrO_2 (sulfite-complex rout)	2.5	Nafion115	1.710	227	S5
Pt/CB	0.5	IrO_2 (colloid method)	3.0	Nafion112	1.615	296	S6
Pt/CB	0.2	IrO_2/SnO_2	1.2	Nafion212	1.600	833	S7
Pt/CB	0.5	IrO_2 (commercial)	3.0	Nafion212	1.564	452	S8

Table S4. List of single cell components.

Components	Specification
Anode catalyst layer	
• MWNT/PBI/Ir	Self-made; Ir loading: 0.5 mg cm^{-2}
• CB/PBI/Ir	Self-made; Ir loading: 0.5 mg cm^{-2}; nafion content: 30 wt%
Electrolyte	Nafion117
Cathode catalyst layer	Pt/C; Pt loading: 0.5 mg/cm^{-2}; nafion content: 30 wt%
Flow field plates	
• Anode plate	Ti
• Cathode plate	Carbon
• Channel width×height×length	1 mm×1 mm×1 mm
• Pattern	Serpentine with 1 mm ribs
Current collectors	
• Anode	Ti sintered compact with Pt plating (Nikko Techno)
• Cathode	SUS316L sintered compact (Nikko Techno)

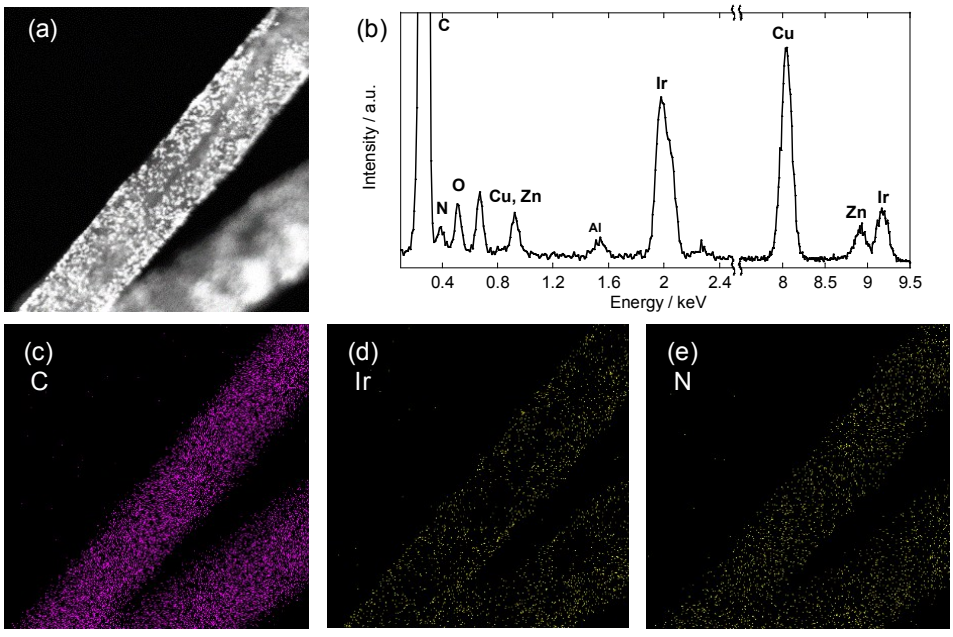

Fig. S1 Elemental mapping of MWNT/PBI/Ir. (a) Dark field transmission electron microscope image of MWNT/PBI/Ir. (b) Energy dispersive X-ray spectrum of the catalyst. Elemental mapping of (c) C, (d) N and (e) Ir of the MWNT/PBI/Ir.

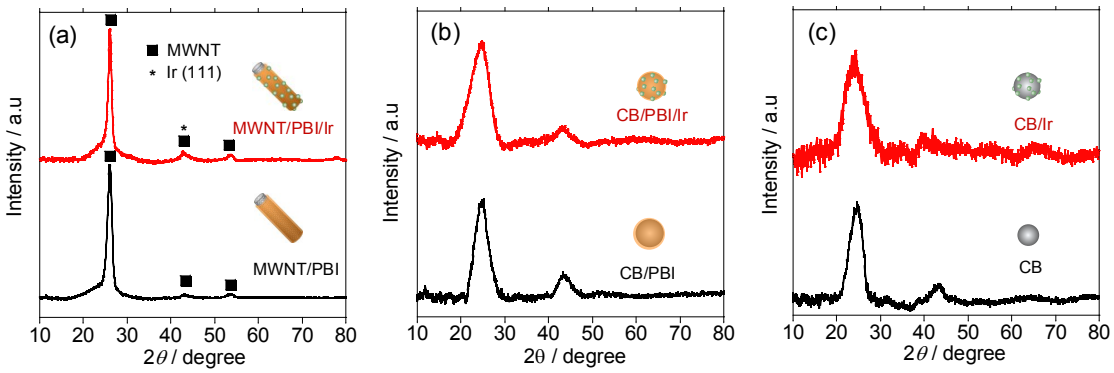

Fig. S2 X-ray diffraction of the catalysts before and after the growth of Ir nanoparticles. XRD patterns of (a) MWNT/PBI (black) and MWNT/PBI/Ir (red), (b) CB/PBI (black) and CB/PBI/Ir (red), and (c) CB (black) and CB/Ir (red).

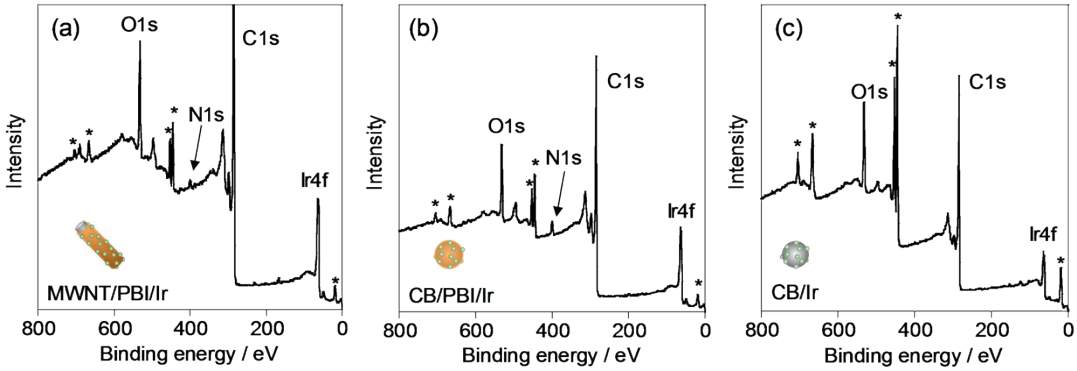

Fig. S3 XPS survey scans of (a) MWNT/PBI/Ir, (b) CB/PBI/Ir and (c) CB/Ir. Asterisks indicate the signal from indium used as the substrate.

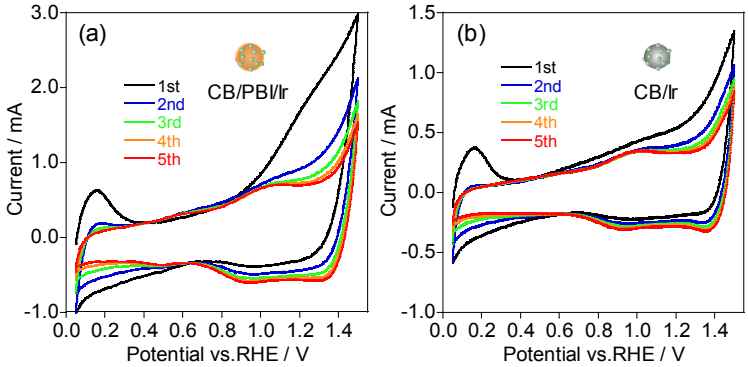

Fig. S4 Electrochemical oxidation of the composites. CV curves for oxidation of (a) CB/PBI/Ir and (b) CB/Ir by potential cycling from +0.05 V to +1.5 V (vs. RHE).

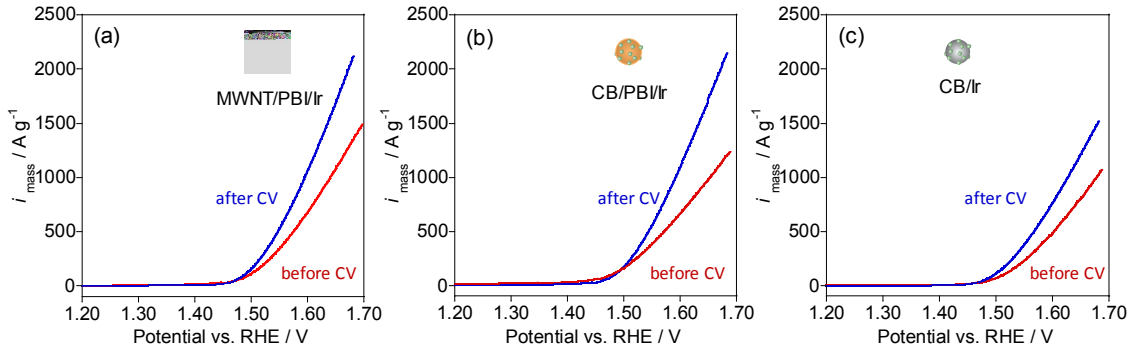

Fig. S5 Comparison of catalytic activity of the catalysts before and after the electrochemical oxidation. LSV curves of the (a) MWNT/PBI/Ir (red) and MWNT/PBI/IrO_x (blue), (b) CB/PBI/Ir (red) and CB/PBI/IrO_x (blue) and (c) CB/Ir (red) and CB/IrO_x (blue) for OER at the scan rate of 5 mV s^{-1}.

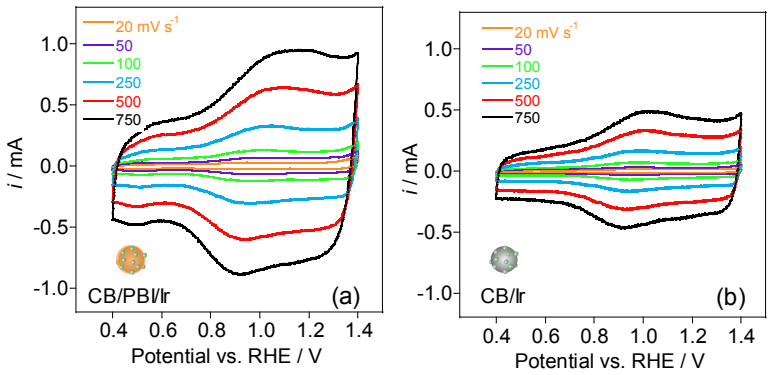

Fig. S6 CV curves of CB/PBI/Ir (a) and CB/Ir (b) at specified scan rates.

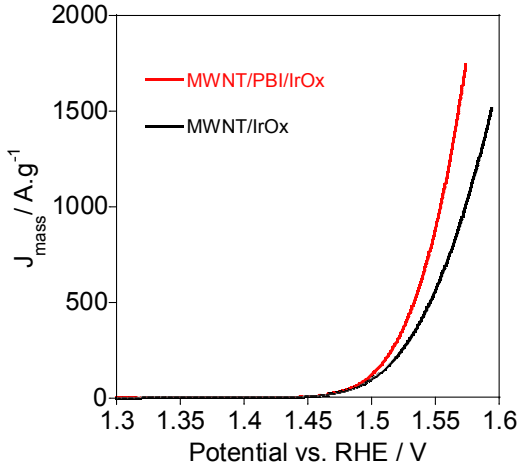

Fig. S7 LSV of the MWNT/PBI/IrO_x (red) and MWNT/IrO_x (black) for OER at the scan rate of 5 mV s^{-1}.

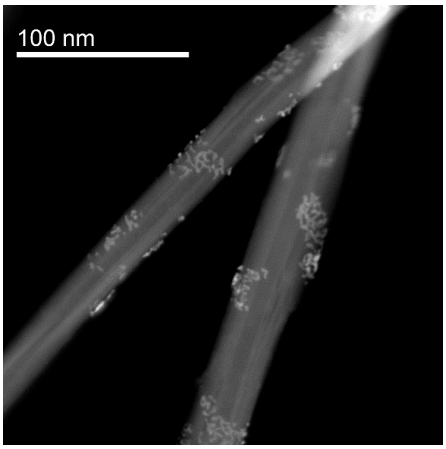

Fig. S8 Dark field STEM image of MWNT/Ir.

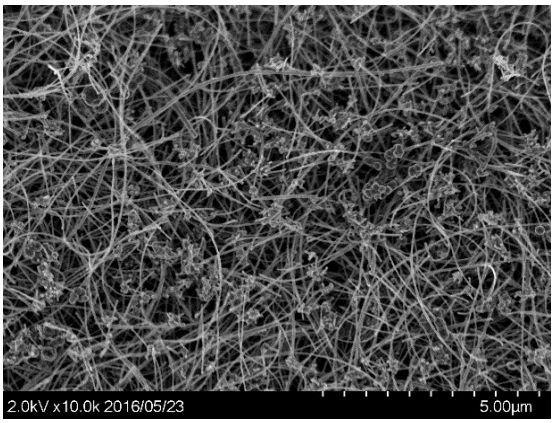

Fig. S9 SEM image of the free-standing anode film of MWNT/PBI/Ir.

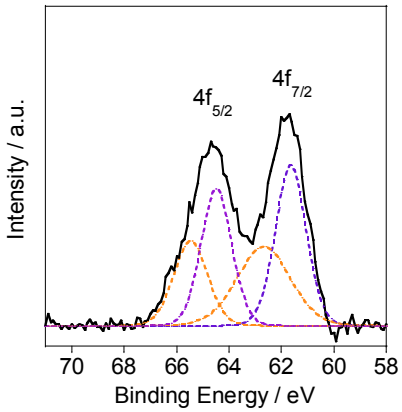

Fig. S10 Electronic state of the Ir nanoparticles after the durability test. XPS spectra of MWNT/PBI/Ir after 100-h durability test at 0.3 A cm^{-2} and 80 °C. Peak deconvolution between Ir(0) and Ir(IV) is shown as the dotted purple and orange, respectively. The ratio between Ir(0) and Ir(IV) was 57 : 43.

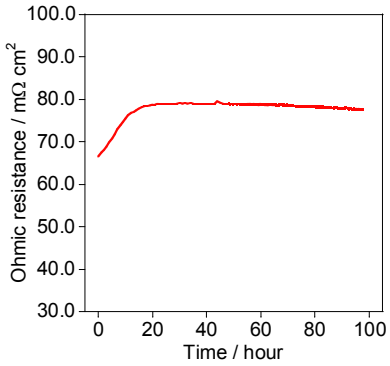

Fig. S11 Time course of the resistance of a PEMWE single cell using MWNT/PBI/Ir anode at 0.3 A cm^{-2} and 80 °C.

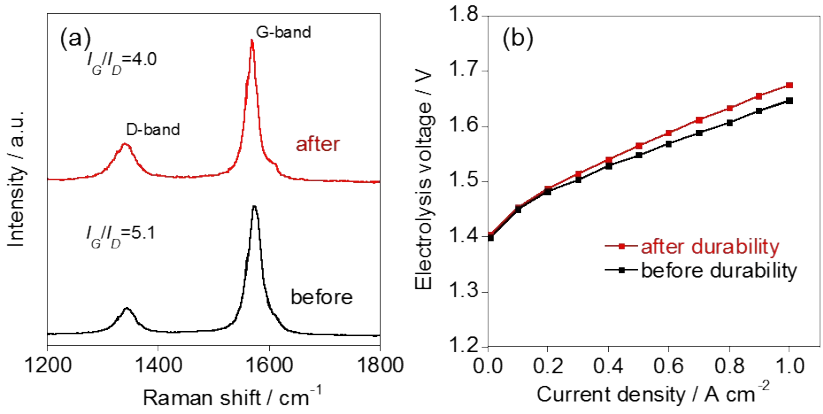

Fig. S12 MEA characterization after the durability test. (a) Raman spectra and (b) I-V curves of MWNT/PBI/Ir at 80 ºC before and after 100-h durability test operated at 0.3 Acm^{-2}.

References

S1. Nong, H. N. *et al.* Oxide-Supported $IrNiO_x$ Core–Shell Particles as Efficient, Cost-Effective, and Stable Catalysts for Electrochemical Water Splitting. *Angew. Chem. Int. Ed.* **54**, 2975-2979 (2015).

S2. Oh, H.-S., Nong, H. N., Reier, T., Gliech, M. & Strasser, P. Oxide-supported Ir nanodendrites with high activity and durability for the oxygen evolution reaction in acid PEM water electrolyzers. *Chem. Sci.* **6**, 3321-3328 (2015).

S3. Lee, Y., Suntivich, J., May, K. J., Perry, E. E. & Shao-Horn, Y. Synthesis and activities of rutile IrO_2 and RuO_2 nanoparticles for oxygen evolution in acid and alkaline solutions. *J. Phys. Chem. Lett.* **3**, 399-404 (2012).

S4. Lim, J. *et al.* Shaped Ir–Ni bimetallic nanoparticles for minimizing Ir utilization in oxygen evolution reaction. *Chem. Commun.* **52**, 5641-5644 (2016).

S5. Siracusano, S. *et al.* Investigation of IrO_2 electrocatalysts prepared by a sulfite-couplex route for the O_2 evolution reaction in solid polymer electrolyte water electrolyzers. *Int. J. Hydrogen Energy* **36**, 7822-7831 (2011).

S6. Song, S. *et al.* Electrochemical investigation of electrocatalysts for the oxygen evolution reaction in PEM water electrolyzers. *Int. J. Hydrogen Energy* **33**, 4955-4961 (2008).

S7. Xu, J., Liu, G., Li, J. & Wang, X. The electrocatalytic properties of an IrO 2/SnO 2 catalyst using SnO 2 as a support and an assisting reagent for the oxygen evolution reaction. *Electrochimica Acta* **59**, 105-112 (2012).

S8. Su, H., Bladergroen, B. J., Linkov, V., Pasupathi, S. & Ji, S. Study of catalyst sprayed membrane under irradiation method to prepare high performance membrane

electrode assemblies for solid polymer electrolyte water electrolysis. *Int. J. Hydrogen Energy* **36**, 15081-15088 (2011).